Case Studies in Chemical and Environmental Engineering 13 (2026) 101358

Contents lists available at ScienceDirect

Case Studies in Chemical and Environmental Engineering

journal homepage: www.sciencedirect.com/journal/case-studies-in-chemical-and-environmental-engineering

Case Report

Electromembrane and pervaporation technologies for the production of highly concentrated formic acid from captured CO_2 valorization

Ainhoa Unzurrunzaga [a], Leire Lorenzo [b], Ainhoa Aguirre [b], María Fernández [b], Yolanda Belaustegui [c,*]

[a] TECNALIA, Basque Research and Technology Alliance (BRTA), Parque Científico y Tecnológico de Gipuzkoa, Mikeletegi Pasealekua, 7, Donostia-Gipuzkoa, 20009, Spain

[b] TECNALIA, Basque Research and Technology Alliance (BRTA), Parque Científico y Tecnológico de Araba, Leonardo Da Vinci Kalea, 11, Miñano Mayor, Araba, 01510, Spain

[c] TECNALIA, Basque Research and Technology Alliance (BRTA), Parque Científico y Tecnológico de Bizkaia, Astondo Bidea, Edif. 700, Derio-Bizkaia, 48160, Spain

ARTICLE INFO

Keywords:
Formic acid
Potassium hydroxide
CO_2 valorization
Electro-membrane technologies
Pervaporation
High concentration

ABSTRACT

Electro-membrane technologies to salt splitting chemicals such as potassium formate generated during the electrochemical conversion of captured CO_2 to obtain formic acid and potassium hydroxide represents a crucial pathway toward carbon neutrality and circular economy. The study demonstrated that the most effective configuration employed two cation exchange membranes (Nafion 324) to separate the anodic, cathodic and central compartments, with the feed solution circulated through the central compartment. This setup enabled potassium ions to migrate to the catholyte, where KOH was concentrated, while protons generated in the anodic compartment moved into the central compartment, maintaining an acidic pH (≈1) and allowing the concentration of formic acid. Optimal performance was achieved at 1500 A m^{-2} and a circulated charge of 0.6715 F, yielding up to 100 g L^{-1} of formic acid and 140 g L^{-1} of potassium hydroxide. Additionally, pervaporation using a PERVAP 4101 membrane successfully broke the formic acid–water azeotrope, reaching concentrations up to 90%. This is the first study that demonstrates the production of highly concentrated formic acid from captured CO_2 by combining electrodialysis with monopolar membranes and pervaporation technologies.

1. Introduction

The enormous amount of anthropogenic carbon dioxide (CO_2) emissions resulting from fossil fuel use has led to severe environmental consequences, such as global warming and climate change, threatening living communities. In 2022, atmospheric CO_2 levels reached 421 ppm and are projected to rise to 790 ppm by 2100 if current industrial emissions continue unchecked [1]. Carbon dioxide capture, utilization and storage (CCUS) technologies are considered promising solutions to reduce CO_2 emissions by converting it into value-added products such as carbon monoxide, hydrocarbons, alcohols (methanol or ethanol), formic acid and formate [2,3].

In the framework of the Horizon Europe WaterProof project (https://www.waterproof-project.eu/), a novel biorefinery concept was developed to electrochemically convert CO_2 emissions from urban waste treatment facilities—such as wastewater treatment plant and consumer waste incineration plant—into valuable green consumer products. The project aims to develop a technology that reduces greenhouse gas (GHG) emissions by transforming CO_2 into formate-derived value-added chemicals, thereby replacing fossil-based feedstocks and promoting industrial electrification. The electrochemical process converts CO_2 into potassium formate (HCOOK), which is subsequently processed into formic acid (HCOOH) and potassium hydroxide (KOH). These products are used in applications such as cleaning detergents, fish leather tanning and acidic deep eutectic solvents (ADES) for metal recovery from wastewater sludge and incineration ash. The entire process is powered by renewable electricity, contributing to a clean water cycle and supporting the transition to a climate-neutral and circular economy.

Formic acid is considered a high-value fine chemical, with a market value exceeding €2.24 billion in 2024 and projected to reach approximately €3.67 billion by 2034 [4]. Currently, the most widely industrial production method involves the carbonylation of methanol with carbon monoxide to form methyl formate, followed by hydrolysis to yield formic acid and methanol. However, this process is energy intensive and

* Corresponding author.
E-mail address: yolanda.belaustegui@tecnalia.com (Y. Belaustegui).

https://doi.org/10.1016/j.cscee.2026.101358
Received 29 September 2025; Received in revised form 18 February 2026; Accepted 27 February 2026
Available online 3 March 2026
2666-0164/© 2026 The Authors. Published by Elsevier Ltd. This is an open access article under the CC BY license (http://creativecommons.org/licenses/by/4.0/).

fossil resource dependent, highlighting the need for more sustainable alternatives [5].

Formic acid is a key intermediate feedstock in the textile, pharmaceutical, and agricultural industries, where it is widely used as a preservative, antibacterial agent and hydrogen carrier [6]. Within the WaterProof Horizon Europe project, formic acid at concentrations of around 80 wt% is employed in the production of cleaning products, fish leather, and acidic deep eutectic solvents (ADES). For these applications, concentrating formic acid up to 80% is essential due to the need for higher purity, enhanced reactivity and improved performance in chemical transformations and industrial formulations [7]. This concentration ensures that the acid meets the technical and functional requirements of its target uses, particularly in processes where diluted formic acid would be less effective or inefficient.

The electrochemical reduction of carbon dioxide (CO_2 ECR) is a promising technology for the selective production of formate or formic acid, with the product distribution influenced by the electrolyte pH [8,9]. Despite its potential, CO_2ECR systems face several limitations, including catalyst stability [10], low selectivity, competing side reactions, and the formation of undesired byproducts [11,12]. Moreover, these systems often lack reliability required for scale up and commercial deployment. An alternative strategy involves the prior capture of CO_2 followed by its electrochemical conversion into potassium formate (HCOOK) [13]. This approach enhances selectivity by minimizing the formation of side products such as carbon monoxide (CO) and hydrogen (H_2), which are commonly observed in direct CO_2 electroreduction. Additionally, it enables the integration of CO_2 capture and conversion into a single process, facilitating electrification and the use of renewable energy sources. The resulting formate can be further processed using electromembrane technologies to produce formic acid (HCOOH) and potassium hydroxide (KOH). These technologies are membrane-based separation processes driven by an applied electrical field across a stack of ion-selective membranes allowing for the clean separation of products and improving their suitability for industrial applications [14].

In this study, various electromembrane processes were explored to obtain aqueous solution of HCOOH and KOH from the HCOOK generated during CO_2 capture from urban waste treatment facilities. The processes evaluated include electrodialysis (ED), electro-electrodialysis (EED or salt splitting) [15] and bipolar membrane electrodialysis (BMED) [16]. Direct ED is a membrane separation process recognized for its exceptional ability to separate, desalinate, and concentrate charge ions from wastewater [17]. It uses an electrical potential difference as a driving force to separate ionic species through ion exchange membranes. The efficiency of ED relies on the selective permeability of these membranes to anions and cations under an applied electric field, enabling the separation of charged species in solution [18]. An ED stack typically consists of cation-exchange membranes (CEM) and anion-exchange membranes (AEM) arranged in a stack between two electrodes which serve as the cathode and anode. EED combines water electrolysis with ion migration through permselective ion exchange membranes to produce acids and bases from their corresponding salts. Generally, EED cells consist of two, three or four compartments separated by AEM and/or CEM. BMED integrates ED with bipolar membranes (BPM), enabling water dissociation into H^+ and OH^- under an applied electrical field, allowing the recovery of acids and bases without the use of chemical reagents [19–21]. The membrane configuration of BMED is mainly divided into three types (BPM-CEM-BPM, BPM-AEM-BPM, and BPM-AEM-CEM-BPM).

A key factor influencing the efficiency of the electromembrane processes is the type of ion exchange membranes (IEMs) used to selectively remove charged species from the feed stream. There are three main types of IEMs: cation exchange membrane (CEM), anion exchange membrane (AEM) and bipolar membrane (BPM) which can be used individually or in combination CEMs and AEMs are commonly used due to their ability to block co-ions (anions and cations, respectively) via Donnan repulsion. Ideal membranes exhibit high permselectivity, low electrical resistance, and strong chemical, thermal and mechanical stabilities. Bipolar membranes, composed of a cation-selective and an anion-selective layer, differ functionally from monopolar membranes. Under reverse potential bias, BPMs can induce the dissociation of water molecules into H^+ and OH^- ions enabling in situ acid and base generation [22–24].

These technologies offer several advantages to produce acids and bases over traditional methods, positioning them as a sustainable alternative to conventional chemical methods. These advantages include lower energy consumption, continuous operation, scalability, minimal use of chemical reagents, fewer by-products generation, and compatibility with other separation processes [25].

Recent studies have demonstrated the effectiveness of these technologies in recovering organic acids, such as lactic acid [26], succinic acid [27], citric acid [28], and formic acid [29]. These studies showed that, for the recovery of weak organic acids, bipolar membranes performed better than monopolar, and the BPM-AEM-BPM arrangement was superior to the BPM-AEM-CEM-BPM because this membrane configuration had lower internal resistance, improving the acid recovery efficiency [30]. Current density was a crucial factor in these systems. High current density meant high voltage and electrical driving force and resulted in a faster ion migration speed. However, if the system exceeded the limit current density, concentration polarization occurred, and the voltage could be too high compromising operation safety [31].

Several studies have reported the conversion of sodium formate to formic acid using the BMED approach [29,32,33]. However, the competitive separation between formate and HCO_3^- through anion-exchange membranes, both of which are weak anions, has not been reported in the literature. In particular, the simultaneous separation and conversion of formate from CO_2 electroreduction products into high-purity and high-concentration formic acid have received little attention [29].

Additionally, the possibility of increasing the concentration of recovered formic acid (initially 10-20 wt%) up to 80 wt% could be studied using pervaporation (PV) technology. PV is a membrane-based separation technique that relies on selective permeation of components through a dense membrane, rather than vapor-liquid equilibrium, making it a more efficient and cost-effective alternative to distillation, especially for separating azeotropic mixtures like the formic acid-water system [34,35].

The performance of a pervaporation membrane is typically assessed using the permeability separation factor, which depends on both the operating conditions of the process and the selectivity of the membranes toward the components in the feed solution. For polymeric membranes, selectivity is calculated by the solubility and diffusivity of each chemical species in solution. In the case of hydrophobic porous membranes, the vapor–liquid equilibrium (VLE) characteristics of the feed components at varying concentrations and temperatures can significantly affect membrane selectivity and overall separation efficiency [34]. Membrane selectivity can be quantified not only through the separation factor but also by analyzing the mass or molar flux of individual components and their relative flux ratios under defined operating conditions.

PV has been widely studied for removing volatile organic compounds (VOCs) from water [36]. Major research has been focused on the recovery of bio-alcohol (such as ethanol and butanol) from aqueous solution using hydrophobic membranes. Despite challenges related to membrane selectivity and long-term stability, PV has also been explored for separating organic/organic mixtures with similar physicochemical properties (aromatic/aliphatic) a critical and energy intensive step in chemical industry [37] as well as from breaking azeotropic mixtures [33].

This study addresses two critical aspects of producing formic acid with high concentration and purity optimizing electrodialysis (ED) performance and overcoming the azeotropic limitation through pervaporation (PV). First, the investigation focuses on the influence of membrane type, stack configuration, and current density on system

performance of the ED system. Key parameters such as the final formic acid and potassium hydroxide concentrations, current efficiency, and circulated charge were evaluated under various conditions to identify the optimal configuration for efficient separation.

Second, the challenge of concentrating formic acid beyond its azeotropic limit is considered. Formic acid and water form a maximum-boiling azeotrope at approximately 77.6 wt%, which restricts conventional distillation since the vapor and liquid phases exhibit identical composition at this point [38]. To overcome this limitation, pervaporation is employed using selective membranes that preferentially allow either formic acid or water to permeate, depending on the membrane type. This approach enables the separation of the azeotropic mixture and facilitates the concentration of formic acid beyond 77.6 wt%, reaching up to 80 wt% or higher, as required for industrial applications [35].

2. Experimental

2.1. Materials

Synthetic potassium formate/potassium bicarbonate solutions simulating the streams generated in the electrochemical conversion pilot were used to obtain formic acid and potassium hydroxide. In particular, the solution was prepared by mixing HCOOK (20 wt%), $KHCO_3$ (5 wt%) and deionized water (https://www.waterproof-project.eu/). All the chemicals used were of analytical grade. Potassium formate (96%), potassium bicarbonate (100%), formic acid (98%), potassium hydroxide (90%) and sulfuric acid (96%) were purchased from Scharlab. Deionized water was used to prepare the solutions.

Neosepta AMX, ACM and CMX commercial grade anion and cation exchange membranes were procured from Eurodia Industrie S.A. Fumasep FAS-30 and Fumasep FAK-30 commercial grade anion, and cation exchange membranes were purchased from Fumatech. Nafion 324 commercial grade cation exchange membrane was acquired from Chemours. Ralex MBP from Membrain S.R.O. PERVAP 4101 commercial hydrophilic pervaporation membrane was acquired from Sulzer.

The properties of the monopolar and bipolar ion exchange membranes used in this research are summarize in (Supplementary information 1) and (Supplementary information 2).

Titanium electrode was acquired from Metakem GmbH and Iridium oxide dimensionally stable electrode (DSA-O_2 (IrO_2/Ti)) was purchased from Electrocell S.A.

2.2. Experimental setup

2.2.1. Electromembrane process setup

A filter-press type electrochemical cell was used to separate formate ions from bicarbonate ions and produce formic acid and potassium hydroxide via electromembrane processes. Four different configurations of the cell were evaluated, varying in the type and number of membranes used, as well as the characteristics of the solutions circulated through the compartments:

- Configuration 1: A three-compartment cell separated by an anion exchange membrane (AEM) and a cation exchange membrane (CEM), arranged between the anode and the cathode (Anode-AEM-CEM-Cathode) (Supplementary information 3).
- Configuration 2: A three-compartment cell separated by a bipolar membrane (BPM), an AEM, a CEM, and another BPM, arranged as Anode-BPM-AEM-CEM-BPM-Cathode (Supplementary information 4).
- Configuration 3: A three-compartment cell separated by a CEM and an AEM, arranged as Anode-CEM-AEM-Cathode (Supplementary information 5).
- Configuration 4: A three-compartment cell separated by two CEMs arranged as Anode-CEM-CEM-Cathode (Supplementary information 6).

Table 1
Cell configuration and corresponding figure number.

Configuration scheme	Figure number
Anode-AEM-CEM-Cathode	Supplementary information 3
Anode-BPM-AEM-CEM-BPM-Cathode	Supplementary information 4
Anode-CEM-AEM -Cathode	Supplementary information 5
Anode-CEM-CEM -Cathode	Supplementary information 6

The electrode and membrane area in all configurations was 20 cm^2. The cation exchange membranes tested included Neosepta CMX, Fumasep FAK-30 and Nafion 324. The anion exchange membranes were Neosepta AMX, Neosepta ACM and Fumasep FAS-30 and bipolar membrane was Ralex MBP (Supplementary information 1 and 2). 316 stainless steel was used as the cathode, while DSA-O_2, titanium and graphite were tested as anodes. A volume of 0.25 L solution was recirculated between each compartment and its corresponding vessels using IWAKI MD-10R magnetic drive pumps.

Electrical current was supplied by a DC power source (Elektro Automatic EA-PS-3040C, 40 A and 40 V). Current and voltage were continuously monitored during operation, and the endpoint of each experiment was determined by a sharp increase in voltage. Temperature was not controlled during the experiments.

The composition of feed solution, consisted of 20% potassium formate and 5% potassium bicarbonate, simulating the concentration of the stream generated from the CO_2 capture process in urban waste treatment facilities (https://www.waterproof-project.eu/).

The cell configurations used in this study, along with their corresponding figure numbers are summarized in Table 1.

2.2.2. Pervaporation setup

Pervaporation (PV) technology was employed to concentrate formic acid (Supplementary information 7).

2.3. Experimental procedures

2.3.1. Electromembrane process

Formate ions were separated from bicarbonate ions to produce formic acid using an electromembrane process under various operating conditions. The effects of parameters such as current density across the membrane stack (250 - 2000 A m^{-2}) and the concentrations of the anolyte and catholyte compartments on the performance of the process were studied. Specifically, the concentrations used were 10 g L^{-1} and 46 g L^{-1} for the anolyte (HCOOH) and 10 g L^{-1} and 56 g L^{-1} for the catholyte (KOH). All the experiments were repeated at least three times.

The concentrations of formic acid (HCOOH), formate ($HCOO^-$) and potassium ions (K^+) were determined using ion chromatography (Metrohm 930 Compact IC Flex Ion Chromatograph equipped with a conductivity detector).

The H^+ concentration was determined by titration with NaOH using methyl orange as an indicator, while the OH^- concentration was titrated with HCl using phenolphthalein as an indicator. The current density (CD, A m^{-2}) was calculated as the applied current (I, A) divided by the effective membrane area (A = 20 cm^2 in this study). The performance of the electromembrane process was evaluated in terms of current efficiency (E_c), which represents the ratio of the number of moles produced or transferred to the number of faradays passed through the system. It was calculated using Equation (1):

$$E_c = \frac{(V_t\, C_t - V_0\, C_0)\, Z\, .F}{I\, .t.\ M}\ 100 \qquad \text{Eq. 1}$$

where C_t and C_0 are the concentrations (g L^{-1}) of HCOOH or KOH at time t and 0 (s), respectively; V_t and V_0 are the volumes (L) at time t and 0 (s), respectively; Z is the absolute valence of the formate ion (Z = 1) or potassium ion (Z = 1); *F* is the Faraday constant (96,485C mol^{-1}); I is the applied current (A); t is the time; and M is the molecular weight.

Table 2
Operating conditions for the three-compartment ED cell. Feed solution: 20% potassium formate and 5% potassium bicarbonate, AEM: Neosepta AMX, CEM: Neosepta CMX, Anode: DSA-O_2, Cathode: 316 stainless steel, [HCOOH] = 10 g L^{-1}, [KOH] = 10 g L^{-1}.

Ref	CD (A m^{-2})	Faradays (F)	$[HCOOH]_{an}$(g L^{-1})	$[KOH]_{cat}$ (g L^{-1})	$[HCOO^-]_{cat}$ (g L^{-1})	%Ec HCOOH	%Ec KOH
1	250	1.0309	32.65	120.53	0.218	11.38	76.92
2	500	0.8506	52.57	148.59	——	32.96	82.92
3	750	0.9280	53.17	124.27	0.025	32.48	93.29
4	1000	0.9364	50.67	120.53	——	29.65	84.64
5	1250	1.2979	34.39	137.07	——	13.38	71.75
6	1400	1.0060	45.01	122.67	——	24.14	83.63

The circulated charge (Q) was calculated following equation (2):

$$Q\,(F) = \frac{I.\,t}{96485} \qquad \text{Eq. 2}$$

where I is the current (A), t is the time (s) and 96,485 is the Faraday constant.

2.3.2. Pervaporation

Pervaporation experiments were performed using a hydrophilic membrane (PERVAP 4101) with an effective area of 124.74 cm^2. They were repeated at least three times. The operating conditions were as follows: 80 °C temperature, 50 L h^{-1} flow rate, 1 bar pressure and 50 mbar vacuum pressure.

The concentrations of formic acid (HCOOH) and formate ($HCOO^-$) were determined by ion chromatography (Metrohm 930 Compact IC Flex Ion Chromatograph equipped with a conductivity detector).

Membrane performance was evaluated using the permeability separation factor and the mass or molar flux rate of individual components through the membrane into the permeate at specific operating conditions.

The permeability separation factor (α) compares the permeabilities of two components (a and b) through the membrane and is defined by Equation (3).

$$\alpha = \frac{[Ca_p/Cb_p]}{[Ca_f/Cb_f]} \qquad \text{Eq. 3}$$

where Ca and Cb are the mass of a (water) and b (formic acid) components, and p and f are permeate and feed solutions, respectively.

The molar flux rate (F) describes the amount of a component passing through the membrane per unit area per unit time, expressed in grams per square meter per hour (g m^{-2} h^{-1}).

$$F\left(\frac{g}{m^2.h}\right) = \frac{m}{A.t} \qquad \text{Eq. 4}$$

where m is the mass of the component, A is the area of the membrane through the component flows and t is the time.

3. Results and discussion

3.1. Electromembrane technologies

In this study, four cell configurations were selected to separate selectively formate ions from a solution of potassium formate and potassium bicarbonate, with the aim of obtaining highly concentrated formic acid. The optimal AEM was chosen to minimize proton leakage while enhancing formate transport. Similarly, the CEM was selected to reduce OH^- leakage and facilitate the splitting process [39]. These configurations are summarized in Table 1.

Supplementary information 3 shows a scheme of the Anode-AEM-CEM-Cathode configuration and the associated mass fluxes. It includes one AEM and one CEM placed between the anode and cathode, forming three compartments. The feed solution (20% HCOOK and 5% $KHCO_3$) was fed through the central compartment. Initially, diluted formic acid (10 g L^{-1}) and potassium hydroxide (10 g L^{-1}) solutions were recirculated from the anodic and cathodic compartments, respectively.

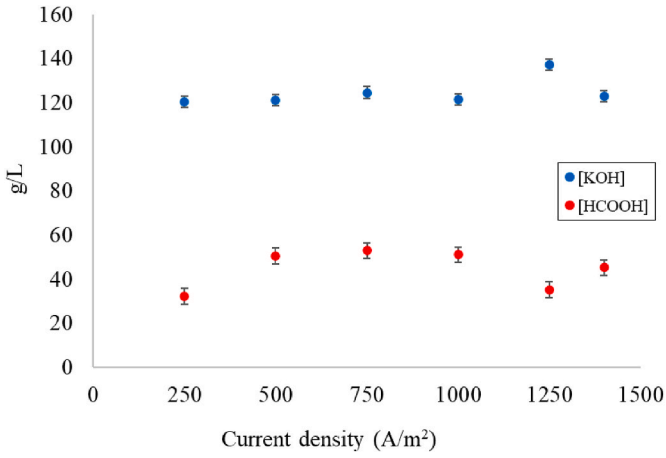

Fig. 1. [HCOOH] and [KOH] (g L^{-1}) vs current density (A m^{-2}) for 1-6 experiments.

Upon applying an electric current, water electrolysis took place, generating oxygen (O_2) and protons (H^+) at the anode and hydrogen (H_2) and hydroxyl ions (OH^-) at the cathode. Formate anions ($HCOO^-$) migrated towards the anode through the AEM and were neutralised by H^+ ions to form formic acid. Simultaneously, potassium ions (K^+) migrated toward the cathode through the CEM and were neutralised by OH^- ions, forming potassium hydroxide. As a result, oxygen and a concentrated formic acid solution were produced in the anodic compartment, while hydrogen and a concentrated potassium hydroxide solution were obtained in the cathodic compartment. In the central compartment, a dilute solution of salts remained. The electrochemical reactions involved in the electrodes and compartments are the following [40]:

Cathode:

$$2\,H_2O + 2\,e^- \rightarrow H_2 + 2OH^-$$

$$OH^- + K^+ \rightarrow KOH$$

Central compartment:

$$HCOOK \rightarrow HCOO^- + K^+$$

$$KHCO_3 \rightarrow HCO_3^- + K^+$$

Anode:

$$2\,H_2O \rightarrow O_2 + 4\,H^+ + 4\,e^-$$

$$HCOO^- + H^+ \rightarrow HCOOH$$

$$HCO_3^- + H^+ \rightarrow H_2CO_3$$

$$H_2CO_3 \rightarrow H_2O + CO_2$$

An initial volume of 0.25 L was circulated through the three

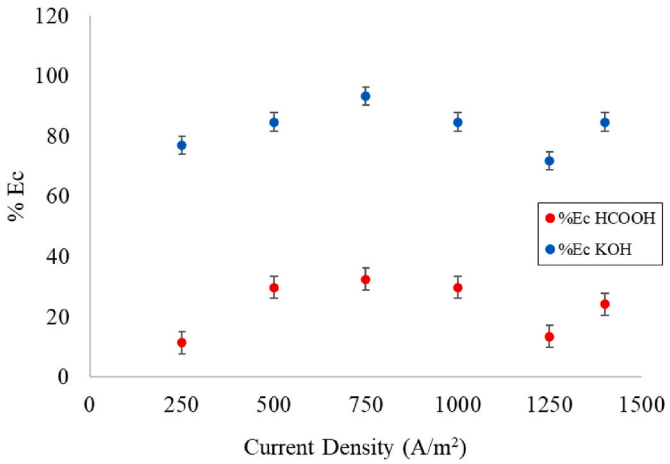

Fig. 2. %Ec HCOOH and %Ec KOH vs current density (A m^{-2}) for 1-6 experiments.

compartments. A DSA-O_2 electrode was used as the anode and 316 stainless steel as the cathode. Neosepta AMX and Neosepta CMX were employed as the anion and cation exchange membranes, respectively. The flow rate was set at 0.6 m^3 h^{-1}.

Table 2 presents the operating conditions for this cell configuration. It was observed that the formic acid solution could only be concentrated by a factor of 2 to 3, whereas potassium hydroxide reached concentration factors of up to 10 (Fig. 1). Regarding current efficiencies (Fig. 2), those corresponding to formic acid remained consistently low across all current densities studied (250 to 1400 A m^{-2}), with the best results observed in the range of 750 to 1000 A m^{-2}. In contrast, potassium hydroxide exhibited higher efficiencies, which were also achieved at the same current density.

However, some discrepancies were observed during the experiments. Specifically, the formate mass balance in experiments 1 to 6 was inconsistent, as the final amount of formate ions was significantly lower than the initial amount. A decrease of approximately 60%-70% was recorded (e.g., in experiment 3, the initial formate mass balance was 40.85 g while the final mass balance was 10.51 g). This loss was likely due to electrooxidation of formate at the anode, caused by the direct contact between formic acid solution and the anode surface. Moreover, the loss was greater at higher current densities, where current efficiencies were lower. Although a dimensionally stable anode (DSA-O_2) was employed, which is designed for oxygen evolution and offering high electrochemical stability, the electrooxidation of formate could not be avoided. This occurred because the formic acid solution was in direct contact with the anode surface, allowing oxidation reactions to proceed at the applied potentials. The catalytic properties of the mixed metal oxides (RuO_2 and IrO_2) that coat the titanium substrate, while beneficial for OER, also promote the oxidation of organic species such as formate, especially at higher current densities [41].

Additionally, electroosmotic flow through both anion and cation exchange membranes led to an increase in the volumes of the anolyte and catholyte. The anion exchange membrane was not selective solely for formate ions, it also allowed bicarbonate ions to pass through. Since both formate and bicarbonate ions are monovalent and similar in size, the membrane could not effectively discriminate between them, resulting in significant bicarbonate crossover. These bicarbonate ions reacted with the H^+ generated at the anode, producing carbonic acid (H_2CO_3). H_2CO_3 is a weak acid and has a very low saturation concentration so most of H_2CO_3 escaped as CO_2. Moreover, a small amount of formate ions crossed the cation exchange membranes into the potassium hydroxide solution.

To improve current efficiency, reduce bicarbonate crossover and minimize electro-osmotic flow, Fumasep FAS-30 and FKS-30 membranes were tested. Neosepta AMX is thicker membrane than FAS-30 so it could decrease ionic path length decreasing ohmic resistance and increase the current density. However, these membranes performed poorly under the process conditions, becoming stretched and damaged even at low current densities (250 A m^{-2}). This was likely due to the alkaline medium (KOH) and the presence of reactive species (H^+, CO_2, formate, bicarbonate), which can degrade the functional groups of the membrane and reduce its structural integrity. Furthermore, although a current density of 250 A m^{-2} may seem low for industrial processes, in systems with thin membranes it can induce localized heating, leading to loss of elasticity and extreme concentration gradients, causing swelling due to water absorption [42].

New experiments were conducted by replacing the DSA-O_2 anode with titanium and graphite anodes in an attempt to improve process efficiency. These alternative materials are more inert and do not catalyze the oxidation of formate to CO_2 and H_2O [33]. Table 3 summarizes the operating conditions and results of these experiments. The current efficiency for formic acid concentration increased slightly from 30% to 37% when using a titanium anode at 500 A m^{-2}, while the current efficiency for potassium hydroxide remained largely unchanged compared to experiments 1 to 6.

However, the same issues persisted: the formate mass balance remained inconsistent, with losses attributed to electrooxidation of formate ions to CO_2 at the anode; there was simultaneous crossover of formate and bicarbonate ions through the anion exchange membrane and a small concentration of formate also crossed the cation exchange membrane.

The graphite was also tested as anode but suffered from corrosion and degradation under the studied conditions, making it unsuitable for this process (Supplementary information 8).

Another strategy to improve the current efficiency involved increasing the concentration of the anolyte and catholyte solution from 10 g L^{-1} to 1 M (46 g L^{-1} formic acid and 56 g L^{-1} potassium hydroxide). Under these conditions, ion transport between the electrodes enhanced, reducing the cell potential and enabling operation at higher current densities. Table 4 summarizes the current efficiency results for different current densities at higher anolyte and catholyte concentrations.

However, the mass balance in these experiments suggested that the formic acid continued to undergo electrooxidation at the anode, regardless of the electrode material used. Furthermore, increasing the anolyte and catholyte concentrations to 1 M did not improve the current efficiencies for either formic acid or potassium hydroxide when compared to the experiments conducted with 10 g L^{-1} solutions.

An alternative three-compartment electrodialysis cell incorporating bipolar membranes was tested with the aim of increasing the formic acid concentration while preventing the oxidation of formate/formic acid in the anodic compartment, as this design avoids direct contact between the formic acid solution and the anode surface (Supplementary information 4). The feed solution was introduced into the central compartment, while diluted solutions of HCOOH and KOH were circulated through the anodic and cathodic compartments, respectively.

Table 3
Operating conditions for the three-compartment ED cell substituting DSA-O_2 anode by titanium. Feed solution: 20% potassium formate and 5% potassium bicarbonate, AEM: Neosepta AMX, CEM: Neosepta CMX, Cathode: 316 stainless steel, [HCOOH] = 10 g L^{-1}, [KOH] = 10 g L^{-1}.

Ref	Anode	CD (A m^{-2})	Faradays (F)	$[HCOOH]_{an}$ (g L^{-1})	$[KOH]_{cat}$ (g L^{-1})	$[Formate]_{cat}$ (mg L^{-1})	%Ec HCOOH	%Ec KOH
7	Titanium	500	0.8158	52	164	0.43	36.94	87.71
8	Titanium	250	0.8316	47	144	1.21	29.16	75.38

Table 4
Operating conditions for the three-compartment ED cell increasing anolyte and catholyte compartment concentration. Feed solution: 20% potassium formate and 5% potassium bicarbonate, AEM: Neosepta AMX, CEM: Neosepta CMX, Anode: Titanium, Cathode: 316 stainless steel, Anolyte: 46 g L^{-1} HCOOH, Catholyte: 56 g L^{-1} KOH.

Ref	CD (A m^{-2})	Faradays (F)	$[HCOOH]_{an}$ (g L^{-1})	$[KOH]_{cat}$ (g L^{-1})	$[Formate]_{cat}$ (mg L^{-1})	%Ec HCOOH	%Ec KOH
9	500	0.8649	59.60	215.79	1.34	20.51	86.20
10	1000	1.0234	64.50	207.20	0.10	20.14	79.11
11	1500	1.0054	69.80	213.55	0.47	20.50	75.03

Table 5
Operating conditions for the four-compartment ED cell with bipolar membranes. Central compartment: Feed solution: 20% potassium formate and 5% potassium bicarbonate, AEM: Neosepta AMX, CEM: Neosepta CMX, BPM: Ralex, Anode: Titanium, Cathode: 316 stainless steel, Anolyte: 10 g L^{-1} HCOOH, Catholyte: 10 g L^{-1} KOH.

Ref	CD (A m^{-2})	Faradays (F)	[HCOOH] (g L^{-1})	[KOH] (g L^{-1})	%Ec HCOOH	%Ec KOH	$[Formate]_{KOH}$ (mg L^{-1})
12	500	0.8692	90.71	104.53	46.46	76.00	2.35

Table 6
Operating conditions for the three-compartment ED circulating feed solution by cathodic compartment. Feed solution: 20% potassium formate and 5% potassium bicarbonate, AEM: Neosepta AMX, CEM: Neosepta CMX, Anode: Titanium, Cathode: 316 stainless steel. Anolyte: 5 g L^{-1} H_2SO_4, Catholyte: Feed solution, Central compartment: 5 g L^{-1} HCOOH.

Ref	CD (A m^{-2})	Faradays (F)	[HCOOH] (g L^{-1})	%Ec HCOOH	$[Formate]_{cat}$ (mg L^{-1})
13	500	0.7818	61.26	31.98	2.01
14	750	0.2845	44.36	69.38	1.39
15	1000	0.2325	37.52	72.69	0.34

Table 7
Operating conditions for the three-compartment ED circulating feed solution by cathodic compartment, adding formic acid to catholyte compartment. Feed solution: 20% potassium formate and 5% potassium bicarbonate, AEM: Neosepta AMX, CEM: Neosepta CMX, Anode: Titanium, Cathode: 316 stainless stee. Anolyte: 5 g L^{-1} H_2SO_4, Catholyte: Feed solution, Central: 5 g L^{-1} HCOOH.

Ref	CD (A m^{-2})	Faradays (F)	[HCOOH] (g L^{-1})	%Ec HCOOH	$[Formate]_{cat}$ (mg L^{-1})
16	500	0.5223	73.60	51.56	1.56
17	1000	0.2984	53.05	80.93	1.36

Formic acid was concentrated by combining H^+ ions, generated in the cationic layer of the bipolar membrane, with formate ions crossing the anion exchange membrane. Similarly, KOH was concentrated by combining OH^- ions generated in the anionic layer of the bipolar membrane with potassium ions crossing the cation exchange membrane.

The current efficiency improved slightly (46% vs 30%) using a Ralex bipolar membrane and applying a current density of 500 A m^{-2} (Table 5). However, as observed by Jaime-Ferrer et al. [32], there was a loss of formic acid due to its diffusion through both the bipolar and anion exchange membranes. Additionally, bicarbonate ions competed with formate ions for transport through the anion exchange membrane, which contributed to a decrease in current efficiency. A small amount of formate ions also crossed the cation exchange membrane.

Moreover, the use of bipolar membranes requires additional energy to drive water dissociation at the bipolar junction, which results in higher cell voltage and increased energy consumption compared to conventional electrodialysis. In addition, the membrane exhibited poor chemical stability under extreme pH conditions, leafing to gradual degradation over time. These limitations must be considered when assessing the feasibility of BPMs for industrial-scale formic acid production.

Considering the low efficiencies for formic acid and the drawbacks of bipolar membranes, an additional cell configuration was studied (Supplementary information 5). In this setup, the feed solution was introduced as the catholyte through the cathodic compartment to maintain a basic pH. This condition favoured the presence of carbonate ions (with two negative charges) over bicarbonate ions (with one negative charge), thereby reducing competition between formate and bicarbonate ions for transport through the anion exchange membrane into the central compartment, where formic acid was concentrated.

Upon applying an electric current between the electrodes, formate ions migrated from the catholyte through the anion exchange membrane into the central compartment and combined with protons originated from the anolyte to form formic acid. The anolyte consisted of 5 g L^{-1} H_2SO_4, while the central compartment was filled with 5 g L^{-1} HCOOH. Titanium was used as the anode and stainless steel 316 as the cathode. The configuration consisted of a three-compartment cell, with one cation exchange membrane (Neosepta CMX) and one anion exchange membrane (Neosepta AMX) placed between the electrodes.

Table 6 summarizes the experimental conditions, and the results obtained with this configuration at different current densities. The data indicates that, as the current density increased, the concentration of formic acid in the central compartment decreased and the current efficiency improved. However, it is important to note that the total charge passed (F) was also lower at higher current densities due to the shorter duration of the experiments. Consequently, the final concentration of formic acid was lower. To achieve higher concentration, the total charge passed would need to be increased.

Among the conditions tested, the highest formic acid concentration (from 5 g L^{-1} to 61 g L^{-1}) was obtained at 500 A m^{-2}. Furthermore, using this cell configuration, the mass balance was consistent, suggesting that the issue of formic acid electrooxidation at the anode had been solved.

However, the pH in the catholyte compartment was extremely basic pH~14 (Supplementary information 9), leading to degradation of the anion exchange membrane and turning the colour of the catholyte solution brown (Supplementary information 10).

Two alternative strategies were proposed to prevent the catholyte compartment from reaching an excessively high pH level (≈14) in this cell configuration. The first approach involved adding a few drops of formic acid to the catholyte (feed solution) to keep the pH at or below 10

Table 8
Operating conditions for the three-compartment ED circulating feed solution by cathodic compartment. Feed solution: 20% potassium formate and 5% potassium bicarbonate, AEM: Neosepta AMX, CEM: Neosepta CMX, Anode: Titanium, Cathode: 316 stainless steel. Anolyte: 10 g L^{-1} H_2SO_4, Catholyte: Feed solution, Central: 5 g L^{-1} HCOOH.

Ref	CD (A m^{-2})	Faradays (F)	[HCOOH] (g L^{-1})	%Ec HCOOH	$[Formate]_{cat}$ (mg L^{-1})
18	500	1.0191	76.67	47.92	1.56
19	750	0.2677	42.73	67.84	1.36

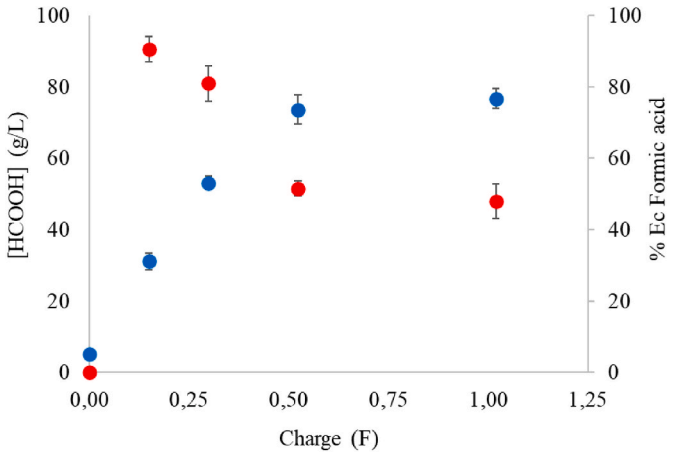

Fig. 3. Effect of the circulated charge (F) on the [HCOOH] (g L^{-1}) and current density (A m^{-2}).

throughout the process, (see results in Table 7). The second approach consisted of increasing the concentration of H_2SO_4 in the anolyte compartment from 5 g L^{-1} to 10 g L^{-1} to enhance the proton flow through the cation exchange membrane into the central compartment, and subsequently into the catholyte. Despite the Neosepta AMX being an anion exchange membrane, a small proportion of protons was able to pass through it (see results in Table 8).

Both strategies, adding formic acid drops to the catholyte solution (to maintain pH $\leq$ 10) and increasing the H_2SO_4 concentration to 10 g L^{-1} in the anolyte, led to improved results. In both cases, the current efficiency for formic acid increased, reaching approximately 81% and 68%, respectively, at a current density of 1000 A m^{-2} and with a similar total charge passed. In either case, formic acid was concentrated up to sevenfold, and its electrooxidation was avoided. However, increasing the H_2SO_4 concentration in the anolyte solution from 5 g L^{-1} to 10 g L^{-1} resulted in degradation of the cation exchange membrane and caused the catholyte solution to turn brown. Additionally, in both scenarios, a small amount of formate ions crossed the cation exchange membrane. It is also worth noting that this cell configuration did not enable KOH production.

Fig. 3 shows the effect of the circulated charge on the concentration of formic acid and the current efficiency of the process. As the circulated charge increased, so did the concentration of formic acid, stabilizing at around 0.50 F. However, the current efficiency decreased as the charge increased. Therefore, it was concluded that the maximum achievable formic acid concentration with this configuration at a circulated charge of 0.50 F was around 70-80 g L^{-1}, with a current efficiency of 50%-60%.

Finally, the Anode-CEM-CEM-Cathode configuration (Supplementary information 6) was tested to address the drawbacks identified in the other configuration studied. In this setup, the feed solution consisting of 20% potassium formate and 5% potassium bicarbonate was circulated through the central compartment. Simultaneously, an aqueous solutions of 5 g L^{-1} sulfuric acid and 5 g L^{-1} potassium hydroxide were circulated through the anodic and cathodic compartments, respectively. Titanium was used as the anode and 316 stainless steel as the cathode. Two cation exchange membranes (Nafion 324) were placed between the electrodes, forming a three-compartment cell. Nafion 324 was selected because its structure combines high proton conductivity with exceptional chemical and thermal stability. These characteristics minimize swelling and enhance durability under harsh operating conditions, resulting in excellent current efficiency, extended service life, and consistent product purity.

Upon application of current, potassium ions from the central compartment migrated through the cation exchange membrane into the catholyte, where potassium hydroxide was concentrated. Concurrently, protons from the anolyte crossed the other cation exchange membrane into the central compartment, acidifying the solution to approximately pH 1. This acidification ensured the formation of CO_2 and increased the concentration of formic acid, removing the bicarbonate ions from the solution, resulting in very high purity formic acid.

Table 9
Operating conditions for the three-compartment EED circulating feed solution by central compartment. Feed solution: 20% potassium formate and 5% potassium bicarbonate, CEM: Nafion 324, Anode: Titanium, Cathode: 316 stainless steel. Anolyte: 5 g L^{-1} H_2SO_4, Catholyte: 5 g L^{-1} KOH, Central: Feed solution.

Ref	CD (A m^{-2})	t (min)	Faradays (F)	pH	$[HCOOH]_{central}$ (g L^{-1})	$[K^+]_{central}$ (mg L^{-1})
20	500	0	0.0000	8.7	100.18	117.84
		427	0.2655	4.3	105.16	64.46
		864	0.5372	3.1	95.74	25.38
21	750	0	0.0000	8.7	100.18	116.18
		427	0.3917	3.7	99.80	48.64
		867	0.8086	1.4	100.27	0.12
22	1000	0	0.0000	8.7	100.18	117.84
		429	0.5335	3.1	113.67	32.54
		889	1.1055	1.3	93.77	0.00
23	1000	0	0.0000	8.7	106.02	114.33
		420	0.5223	3.2	113.24	33.56
		600	0.7461	1.8	111.97	3.97
		840	1.1045	1.6	106.56	0.00
24	1500	0	0.0000	8.7	108.42	116.28
		420	0.7834	1.7	110.54	0.00
		510	0.9513	1.3	109.75	0.00
		600	1.1192	1.3	102.80	0.00
25	1500	0	0.0000	8.7	108.42	116.28
		120	0.2238	4.8	104.36	78.08
		180	0.3358	4.1	101.58	57.07
		240	0.4477	3.5	103.91	39.66
		300	0.5596	3.1	101.36	23.98
		360	0.6715	1.9	102.03	0.00
		420	0.7834	1.4	104.19	0.00
26	2000	0	0.0000	8.7	108.42	116.28
		60	0.1492	5.4	97.00	76.55
		120	0.2984	4.3	101.87	62.21
		180	0.4477	3.6	103.96	42.01
		240	0.5969	2,9	91.14	17.55
		300	0.7461	1.5	100.93	0.00
		360	0.8953	1.3	105.54	0.00

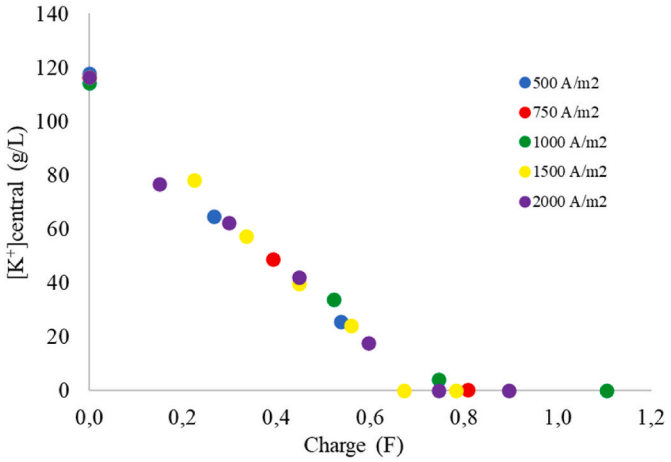

Fig. 4. Effect of circulated charge (F) in the potassium ions removal from the central compartment depending on current density (A m^{-2}).

Table 9 presents the results obtained at various current densities and time intervals, aimed at determining the total charge passed and the pH of the central solution once potassium ions were completely removed. The effect of the circulated charge on potassium ion removal from the central compartment at different current densities is shown in Fig. 4, while the relationship between pH and potassium ion concentration in the central compartment is illustrated in Fig. 5.

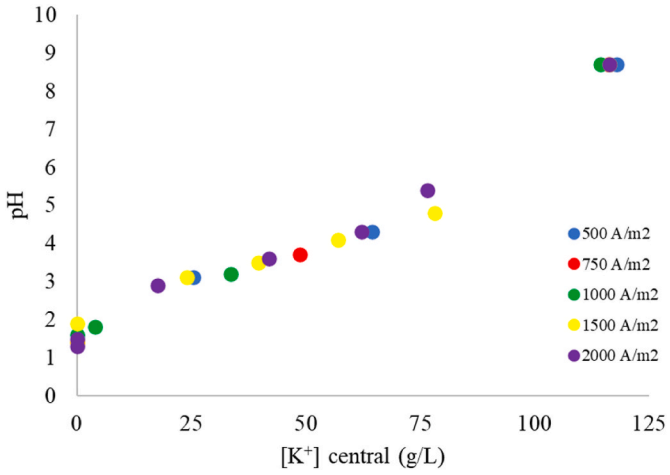

Fig. 5. pH vs potassium concentration in central compartment.

Table 10
Different cell configurations to obtain formic acid.

Ref. Cell Configuration	Current Density (A m^{-2})	Faradays (F)	[HCOOH] (g L^{-1})	[KOH] (g L^{-1})
Supplementary information 3	500	0.8158	52	164
Supplementary information 4	500	0.8692	91	105
Supplementary information 5	500	0.5223	74	——
Supplementary information 6	1500	0.6715	110	140

As shown in Fig. 4, potassium ions removal increased with the total charge circulated. This behavior was strongly influenced by the applied current density, with the most efficient removal observed at 1500 A m^{-2}. At this current density, the migration of potassium ions through the cation exchange membrane into the catholyte was maximized. Furthermore, when the pH of the central compartment decreased to between 1 and 2, the concentration of potassium ions in this compartment effectively dropped to zero, indicating complete migration. This acidification facilitated the formation of CO_2 and the accumulation of formic acid in the central compartment. The maximum concentration of formic acid achieved was approximately 100 g L^{-1}, while the maximum concentration of potassium hydroxide obtained in the cathodic compartment reached around 140 g L^{-1}. Besides, the membranes were not degraded.

Table 11
Operating conditions for the PV cell. Feed: FA 100 g L^{-1}, Membrane: PERVAP 4101, Flow: 50 L h^{-1}, Pressure: 1 bar, membrane area: 124.74 cm^2, temperature = 80 °C.

t (min)	Feed (wt%) FA	Permeate (wt%) FA	α_{ab} H_2O/FA	kg $m^{-2}h^{-1}$ (H_2O)	kg $m^{-2}h^{-1}$ (FA)	H_2O/FA Ratio
0	11.34	——	——	——	——	——
10	12.06	0.27	51.04	14.57	0.0391	372.27
20	12.51	1.12	12.58	10.55	0.1199	87.98
30	12.90	1.57	9.27	8.59	0.1372	62.58
50	13.76	2.00	7.81	6.68	0.1364	48.95
70	13.17	2.22	6.68	6.16	0.1399	44.03
90	13.50	2.40	6.34	5.86	0.1443	40.60
120	13.52	2.58	5.90	5.44	0.1440	37.74
150	15.01	2.71	6.35	5.28	0.1468	35.94
180	14.57	2.81	5.89	5.13	0.1484	34.54
210	15.99	2.90	6.37	5.01	0.1497	33.45
240	16.45	2.98	6.41	4.93	0.1513	32.57
270	16.28	3.04	6.20	4.87	0.1527	31.88
301	17.08	3.10	6.43	4.82	0.1543	31.24
334	16.72	3.49	5.55	4.84	0.1752	27.62
360	17.49	3.55	5.75	4.85	0.1787	27.14
390	17.65	3.80	5.,42	4.88	0.1929	25.31
420	17.34	3.95	5.10	4.86	0.2002	24.29
450	18.05	4.01	5.27	4.86	0.2030	23.91
483	18.79	4.09	5.43	4.82	0.2055	23.46
510	19.85	4.15	5.72	4.80	0.2079	23.11
547	20.65	4.23	5.89	4.78	0.2114	22.62
583	21.22	4.33	5.94	4.75	0.2153	22.07
602	21.88	4.37	6.13	4.73	0.2159	21.88
647	23.46	4.56	6.41	4.71	0.2251	20.93
660	23.46	4.61	6.35	4.72	0.2279	20.71
690	24.45	4.72	6.53	4.69	0.2328	20.17

The last configuration tested in the study, Anode-CEM-CEM-Cathode, with central feed solution circulation, Nafion 324 cation exchange membranes, a titanium anode, and a 316 stainless steel cathode—was considered the most effective. The current efficiency for formic acid reached 50–60%, representing a substantial improvement over previous configurations that only achieved 30%–40%. Moreover, acidifying the central compartment to pH 1-2 was crucial to promote the formation of CO_2 from bicarbonate ions and to enhance formic acid concentration by ensuring that formate ions remained in the central compartment and combined with the protons, resulting in high purity formic acid free of bicarbonate ions. Additionally, this configuration uses only cation exchange membranes, improving the simplicity and scalability of the process by avoiding the complexity associated with bipolar membranes or anion exchange membranes.

A summary of the best results obtained from the various cell configurations tested for the concentration of formic acid and potassium hydroxide is provided in Table 10.

In the traditional salt splitting process (Supplementary information 3), formate ions successfully crossed the anion exchange membrane. However, these ions underwent electrooxidation in the anode, making this configuration ineffective for the concentration of formic acid in the anolyte solution. This indicates that the formic acid solution must not be in direct contact with the anode to prevent electro-oxidation.

A second configuration was developed incorporating bipolar membranes (Supplementary information 4), aimed at preventing the electrooxidation of formate ions. This design significantly improved formic acid concentration, achieving up to a tenfold increase. Nevertheless, electrooxidation still occurred to some extent, and the use of bipolar membranes presented challenges for scale-up applications.

The third configuration (Supplementary information 5) allowed the concentration of formic acid up to 74 g L^{-1}, which could be further increased by raising the circulated charge. However, maintaining the pH below 10 required the manual addition of formic acid drops to the catholyte, which proved labor-intensive. Besides, this setup did not allow for potassium hydroxide recovery, led to degradation of the anion exchange membrane, and resulted in a brown-colored catholyte solution.

Considering the limitations of the previous designs and based on the results summarized in Table 10, the most effective configuration was the one employing two cation exchange membranes, with the feed solution circulating through the central compartment (Supplementary information 6). In this arrangement, potassium ions migrated to the catholyte, where KOH was concentrated, while protons produced in the anodic compartment migrated into the central compartment, maintaining an acidic pH and enabling the concentration of formic acid and CO_2. In this configuration 5 g L^{-1} sulfuric acid and 5 g L^{-1} potassium hydroxide were circulated through the anodic and cathodic compartments, respectively. Titanium was used as the anode, 316 stainless steel as the cathode and two Nafion 324 cation exchange membranes were placed between the electrodes. Under these conditions, it was possible to obtain solutions containing approximately 110 g L^{-1} formic acid and 140 g L^{-1} potassium hydroxide, operating at a current density of 1500 A m^{-2} and a circulated charge of 0.6715 F. This is the first time high-purity formic

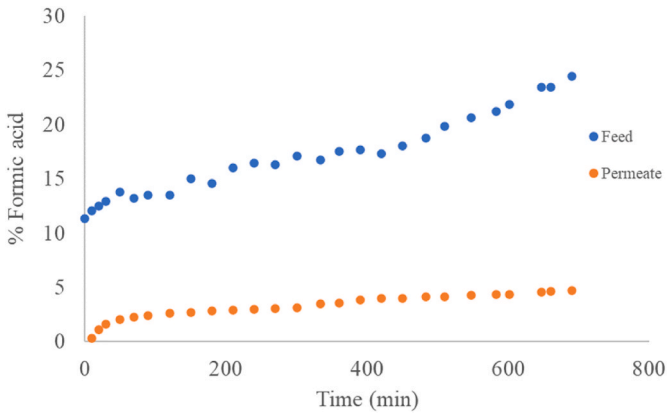

Fig. 6. Formic acid concentration in feed and permeate solution vs time.

acid and potassium hydroxide have been obtained from a formate/bicarbonate solution using cationic membranes, while avoiding bipolar and anionic membranes, and achieving a high current efficiency (50%-60%).

3.2. Pervaporation

Pervaporation (PV) technology was evaluated as a method to concentrate formic acid from 10% to up to 80% (Supplementary information 7). This membrane-based separation process is particularly well suited for concentrating organics compounds from aqueous solutions and for breaking azeotropes. It is commonly used for the separation of binary or multicomponent liquid mixtures. The driving force for the mass transfer of permeants from the feed side to the permeate side of the membrane is the difference in chemical potential of the components across the membrane, typically achieved by reducing the partial pressure on the permeate side using a vacuum pump [43]. The laboratory scale PV setup used in this study is illustrated in Supplementary information 11.

To carry out the pervaporation process, the membrane feed tank was filled with the feed mixture. Once the desired temperature was reached, a vacuum was applied to the permeate side of the membrane module. Permeate samples were collected over time using a cooling trap. The portion of vapor that did not permeate the membrane, referred to as the retentate vapor, was recirculated into the liquid phase of the reactor. The experiment was terminated either after a predetermined duration or upon reaching a target water concentration in the feed solution.

The experiments were conducted using PERVAP 4101 hydrophilic membrane, which selectively facilitates the transport of water to the permeate side under the conditions described in the experimental section. Table 11 summarizes the operating conditions and the results obtained from the pervaporation experiments using 100 g L^{-1} formic acid solution. The results showed an increase of 2.16 % in formic acid concentration in the feed solution. The permeability separation factor was calculated to be 6.53 and the water flow was approximately 370 times higher than the formic acid flow within the first 30 minutes, reaching a ratio of 20 after 420 minutes and stabilizing thereafter.

Fig. 6 illustrates the evolution of formic acid in the feed (retentate) and permeate solutions over the course of the experiment. The formic acid concentration increased in the feed solution, while it stabilized at around 4.5% in the permeate. This membrane exhibits a high degree of cross-linking and tight polymer chain packing, contributing to its selective permeability characteristics.

A multi-stage pervaporation process using the PERVAP 4101 membrane was implemented to achieve high concentrations of formic acid, up to 80% (Table 12). This stepwise concentration approach demonstrated the capability to break the formic acid-water azeotrope, reaching a concentration of 91.34% formic acid (Fig. 7). As the formic acid solution becomes more concentrated, the drag effect increases, resulting in a greater amount of formic acid permeating the membrane along with water. This phenomenon becomes particularly significant near the azeotropic point, where separation becomes more challenging due to the increased volatility of formic acid.

These results demonstrated that it was possible to break the formic acid-water azeotrope and achieve concentrations of up to 90% formic acid in the feed solution or retentate using pervaporation. An alternative strategy could involve a hybrid separation process, where distillation is first used to concentrate formic acid to 50%-60% followed by pervaporation to surpass the azeotropic point and reach concentrations of 80% or higher. This combined approach could offer a more energy efficient and scalable solution to produce highly concentrated formic acid.

4. Conclusions

Electro-membrane technologies proved to be a viable method for producing concentrated formic acid and potassium hydroxide from the formate salts generated in an electrochemical CO_2 conversion process. However, the performance strongly depends on cell configuration. Traditional salt-splitting achieved moderate concentrations but suffered from severe formate oxidation and low efficiency. Bipolar membrane ED improved acid concentration but introduced high energy demand and stability issues. The most effective configuration was the

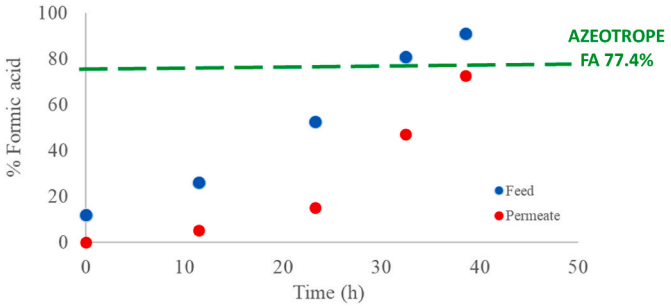

Fig. 7. Formic acid concentrating by pervaporation.

Table 12
Multi-stage pervaporation to concentrate formic acid from 10 % to 80%. Operating conditions for the PV cell. Feed: FA 10 gL^{-1}, Membrane: PERVAP4101, Flow: 50 L h^{-1}, Pressure: 1 bar, membrane area: 124.74 cm^2, temperature: 80 °C.

Step	t (min)	Feed V (g)	Feed (wt%) FA	Permeate V (g)	Permeate (wt%) FA	α_{ab} H_2O/FA	kg m^{-2} h^{-1} (H_2O)	kg m^{-2} h^{-1} (FA)	H_2O/FA Ratio
1	0	1023	12.0	0	—	—	—	—	—
	690	273	26.4	750	5.4	6.3	4.8	0.3	17.6
2	0	1056	25.6	0	—	—	—	—	—
	708	281	52.6	775	15.2	6.2	4.5	0.8	5.6
3	0	1109	54.6	0	—	—	—	—	—
	551	122	81.0	988	47.3	4.8	4.5	4.1	1.1
4	0	1154	81.6	0	0	—	—	—	—
	365	281	91.3	790	72.9	3.9	2.9	7.9	0.4

Anode–CEM–CEM–Cathode setup using Nafion 324 membranes, which delivered up to 110 g L^{-1} formic acid and 140 g·L^{-1} KOH with improved current efficiency (50%–60%), excellent membrane stability, and simplified design, making it the most promising for scale-up.

The pervaporation process was employed to concentrate formic acid, thereby overcoming the azeotropic limitation of formic-acid–water mixtures and successfully increasing concentration to 90 wt%. A hybrid separation strategy combining distillation (to 50–60 wt%) followed by pervaporation (to ≥80 wt%) could be proposed as an energy-efficient and scalable approach for producing high concentration of formic acid suitable for industrial applications.

Overall, the integrated ED–PV methodology offers a sustainable and competitive pathway for highly concentrated formic acid production from captured CO_2, if energy optimization, membrane durability, and economic feasibility are addressed in future work.

CRediT authorship contribution statement

Ainhoa Unzurrunzaga: Data curation, Formal analysis, Investigation, Writing – review & editing. **Leire Lorenzo:** Data curation, Formal analysis, Investigation. **Ainhoa Aguirre:** Data curation, Formal analysis, Investigation. **María Fernández:** Project administration, Resources, Writing – review & editing. **Yolanda Belaustegui:** Conceptualization, Data curation, Formal analysis, Investigation, Methodology, Project administration, Supervision, Visualization, Writing – original draft, Writing – review & editing.

Declaration of competing interest

The authors declare no known conflict of interest.

Acknowledges

This work has received funding from the European Union's Horizon Europe research and innovation programme under grant agreement no. 101058578 (WaterProof). This output reflects the views only of the authors and the European Union cannot be held responsible for any use which may be made of the information contained therein.

Appendix A. Supplementary data

Supplementary data to this article can be found online at https://doi.org/10.1016/j.cscee.2026.101358.

Data availability

Data will be made available on request.

References

[1] Y.-Q. Geng, Y.-X. Guo, B. Fan, F.-Q. Cheng, H.-G. Cheng, Research progress of calcium-based adsorbents for CO_2 capture and anti-sintering modification, J. Fuel Chem. Technol. 49 (2021) 998–1013, https://doi.org/10.1016/S1872-5813(21)60040-3.

[2] M. Bui, et al., Carbon capture and storage (CCS): the way forward, Energy Environ. Sci. 11 (2018) 1062–1176, https://doi.org/10.1039/c7ee02342a.

[3] W. Gao, S. Liang, R. Wang, Q. Jiang, Y. Zhang, Q. Zheng, B. Xie, C.Y. Toe, X. Zhu, J. Wang, Industrial carbon dioxide capture and utilization: state of the art and future challenges, Chem. Soc. Rev. 49 (2020) 8584–8686, https://doi.org/10.1039/d0cs00025f.

[4] Precedence Research, Formic Acid Market, 2025. Retrieved from, https://www.precedenceresearch.com/formic-acid-market.

[5] A.D. Bulushev, J.R.H. Ross, Towards sustainable production of formic acid, ChemSusChem 11 (2018) 821–836, https://doi.org/10.1002/cssc.201702075.

[6] ChG. Okoye-Chine, K. Otun, N. Shiba, Ch Rashama, S.N. Ugwu, H. Onyeaka, ChT. Okeke, Conversion of carbon dioxide into fuels—A review, J. CO2 Util. 62 (2022) 102099, https://doi.org/10.1016/j.jcou.2022.102099.

[7] Chemneo, Efficient formic acid solutions for industrial cleaning challenges, Retrieved from, https://chemneo.com/28393, 2025.

[8] Z. Yang, Y. Jin, Z. Feng, P. Luo, Ch Feng, Y. Zhou, X. An, X. Hao, A. Abudula, G. Guan, Rational strategies for preparing highly efficient Tin-, Bismuth- or indium-based electrocatalysts for electrochemical CO_2 reduction to formic acid/formate, ChemSusChem 16 (2025) e202401181, https://doi.org/10.1002/cssc.202401181.

[9] X. Han, Q. Wang, Y. Wu, C. Wu, Boosting formate production from CO_2 electroreduction over gas diffusion electrode with accessible carbon mesopores, Electrochim. Acta 402 (2022) 139526, https://doi.org/10.1016/j.electacta.2021.139526.

[10] K. Van Daele, B. De Mot, M. Pupo, N. Daems, D. Pant, R. Kortlever, T. Breugelmans, Sn-based electrocatalyst stability: a crucial piece to the puzzle for the electrochemical CO_2 reduction toward formic acid, ACS Energy Lett. 6 (2021) 4317–4327, https://doi.org/10.1021/acsenergylett.1c02049.

[11] X. Long, Y. Peng, Z. Yu, Y. Zhang, X. Jiang, H. Yang, Progress of advanced electrocatalysts towards electrochemical selectivity reduction CO_2 to formic acid, Appl. Catal. Gen. 70 (2025) 120330, https://doi.org/10.1016/j.apcata.2025.120330.

[12] S.A. Al-Tamreh, M.H. Ibrahim, M.H. El-Naas, J. Vaes, D. Pant, A. Benamor, A. Amhamed, Electroreduction of carbon dioxide into formate: a comprehensive review, Chemelectrochem 8 (2021) 3207–3220, https://doi.org/10.1002/celc.202100438.

[13] I. Sullivan, A. Goryachev, I.A. Digdaya, X. Li, H.A. Atwater, D.A. Vermaas, Ch Xiang, Coupling electrochemical CO_2 conversion with CO_2 capture, Nat. Catal. 4 (2021) 952–958, https://doi.org/10.1038/s41929-021-00699-7.

[14] L. Handojo, A.K. Wardani, D. Regina, C. Bella, M.T.A.P. Kresnowati, I.G. Wenten, Electro-membrane processes for organic acid recovery, RSC Adv. 9 (2019) 7854, https://doi.org/10.1039/c8ra09227c.

[15] T. Benvenuti, A. Giacobbo, C.D.M.D. Trindade, K. Santana-Barros, T. Scarazzato, Electrodialysis, electrodialysis reversal and capacitive deionization technologies, Advancement in Polymer-Based Membranes for Water Remediation (2022) 505–539, https://doi.org/10.1016/B978-0-323-88514-0.00014-0.

[16] R. Zhou, Z. Dong, X. Ma, L. Xue, J. Liu, J. He, W. Li, L. Sun, Ch Li, H. Haiyang Yan, Revisiting bipolar membrane electrodialysis for the production of monoprotic organic acids with different pKa and Mw, Chem. Eng. J. 505 (2025) 159125, https://doi.org/10.1016/j.cej.2024.159125.

[17] H. Tang, X. Wang, X. Zhao, Y. Dong, B. Xu, L. Wang, Ion migration characteristics during the bipolar membrane electrodialysis treatment of concentrated reverse osmosis brine, Desalination 561 (2023) 116660, https://doi.org/10.1016/j.desal.2023.116660.

[18] M. Figueira, J. López, M. Reig, J.L. Cortina, C. Valderrama, Techno-economic analysis of seawater reverse osmosis brines treatment using nanofiltration modelling tools, Desalination 568 (2023) 117013, https://doi.org/10.1016/j.desal.2023.117013.

[19] I.G. Wenten, K. Khoiruddin, M.A. Alkhadra, H. Tian, M.Z. Bazan, Novel ionic separation mechanisms in electrically driven membrane processes, Adv. Colloid Interface Sci. 284 (2020) 102269, https://doi.org/10.1016/j.cis.2020.102269.

[20] G. Hopsort, Q. Cacciuttolo, D. Pasquier, Electrodialysis as a key operating unit in chemical processes: from lab to pilot scale of latest breakthroughs, Chem. Eng. J. 494 (2024) 153111, https://doi.org/10.1016/j.cej.2024.153111.

[21] Y. Luo, Y. Liu, J. Shen, B. Van der Bruggen, Application of bipolar membrane electrodialysis in environmental protection and resource recovery: a review, Membranes 12 (2022) 829, https://doi.org/10.3390/membranes12090829.

[22] Ch Huang, T. Xu, Y. Zhang, Y. Xue, G. Chen, Application of electrodialysis to the production of organic acids: state-of-the-art and recent developments, J. Membr. Sci. 288 (2007) 1–12, https://doi.org/10.1016/j.memsci.2006.11.026.

[23] H. Strathmann, A. Grabowski, G. Eigenberger, Ion-exchange membranes in the chemical process industry, Ind. Eng. Chem. Res. 52 (2013) 10364–10379, https://doi.org/10.1021/ie4002102.

[24] M. Wang, B. Xu, Q. Zou, X. Dong, R. Shao, J. Qiao, Graphene oxide prompted double-crosslinked poly(vinyl alcohol)/poly(diallyldimethylammonium chloride) anion-exchange membrane for superior CO_2 electrochemical reduction, Separation and Purification Technology 307 (2023) 122792, https://doi.org/10.2139/ssrn.4273738.

[25] Y. Belaustegui, M.C. Villarán, B. Valle, R. Marquínez, C. García Balboa, J.R. Ochoa, Electromembrane technologies. Some examples of application for recovery of raw materials in industrial waste waters, Trends in electrochemistry and corrosion at the beginning of the 21st century-Homenaje Prof. Costa, Collecció Homenatges, UB (2004).

[26] Q. Wang, G.Q. Chen, L. Lin, X. Li, S.E. Kentish, Purification of organic acids using electrodialysis with bipolar membranes (EDBM) combined with monovalent anion selective membranes, Separation and Purification Technology 279 (2021) 119739, https://doi.org/10.1016/j.seppur.2021.119739.

[27] M. Szczygiełda, K. Prochaska, Alpha-ketoglutaric acid production using electrodialysis with bipolar membrane, J. Membr. Sci. 536 (2017) 37–43, https://doi.org/10.1016/j.memsci.2017.04.059.

[28] X. Sun, H. Lu, J. Wang, Recovery of citric acid from the fermented liquid by bipolar membrane electrodialysis, J. Clean. Prod. 143 (2017) 250–256, https://doi.org/10.1016/j.jclepro.2016.12.118.

[29] Z. Wang, J. Yan, H. Wang, W. Fu, D. He, B. Wang, Y. Wang, T. Xu, Separation and conversion of CO_2 reduction products into high-concentration formic acid using bipolar membrane electrodialysis, J. Membr. Sci. 708 (2024) 123016, https://doi.org/10.1016/j.memsci.2024.

[30] C. Huang, T. Xu, Y. Zhang, Y. Xue, G. Chen, Application of electrodialysis to the production of organic acids: state-of-the-art and recent developments, J. Membr. Sci. 288 (2007) 1–12, https://doi.org/10.1016/j.memsci.2006.11.026.

[31] Y. Sun, Y. Wang, Z. Peng, Y. Liu, Treatment of high salinity sulfanilic acid wastewater by bipolar membrane electrodialysis, Separation and Purification Technology 281 (2022) 119842, https://doi.org/10.1016/j.seppur.2021.119842.

[32] J.S. Jaime-Ferrer, E. Couallier, Ph Viers, G. Durand, M. Rakib, Three-compartment bipolar membrane electrodialysis for splitting of sodium formate into formic acid and sodium hydroxide: role of diffusion of molecular acid, J. Membr. Sci. 325 (2008) 528–536, https://doi.org/10.1016/j.memsci.2008.07.059.
[33] D. Ewis, M. Arsalan, M. Khaled, D. Pant, M.M. Ba-Abbad, A. Amhamed, M.H. El-Naas, Electrochemical reduction of CO_2 into formate/formic acid: a review of cell design and operation, Separation and Purification Technology 316 (2023) 123811, https://doi.org/10.1016/j.seppur.2023.123811.
[34] J.J. Kaczur, L.J. McGlaughlin, P.S. Lakkaraju, Investigating pervaporation as a process method for concentrating formic acid produced from carbon dioxide, Journal of Carbon Research 6 (2020) 42, https://doi.org/10.3390/c6020042.
[35] P. Luis, Fundamental modelling of membrane systems, Membrane and Process Performance (2018) 71–102, https://doi.org/10.1016/B978-0-12-813483-2.00003-4.
[36] H. Potocnik, Y. Smick, I. Plazl, P. Znidarsi Plazl, R. Ambrozic, Model-based design of a microfluidic pervaporation device for intensified VOC separation, Separation and Purification Technology 378 (2025) 134795, https://doi.org/10.1016/j.seppur.2025.134795.
[37] A. Halloub, W. Kujawski, Recent advances in polymeric membrane integration for organic solvent mixtures separation: mini-review, Membranes 15 (2025) 329, https://doi.org/10.3390/membranes15110329.
[38] B. Mahida, H. Benyounes, W. Shen, Process analysis of pressure-swing distillation for the separation of formic acid–water mixture, Chem. Pap. 75 (2021) 599–609, https://doi.org/10.1007/s11696-020-01329-5.
[39] F. Habibzadeh, P. Mardle, N. Zhao, H.D. Riley, D.A. Salvatore, C.P. Berlinguette, S. Holdcroft, Z. Shi, Ion exchange membranes in electrochemical CO_2 reduction processes, Electrochem. Energy Rev. 6 (2023) 26, https://doi.org/10.1007/s41918-023-00183-9.
[40] M.S. Sajna, S. Zavahir, A. Popelka, P. Kasak, A. Al-Sharshani, U. Onwusogh, M. Wang, H. Park, D.S. Han, Electrochemical system design for CO_2 conversion: a comprehensive review, J. Environ. Chem. Eng. 11 (2023) 110467, https://doi.org/10.1016/j.jece.2023.110467.
[41] Y. Li, M.-S. Yao, Y. He, S. Du, Recent advances of electrocatalysts and electrodes for direct formic acid fuel cells: from nano to meter scale challenges, Nano-Micro Lett. 17 (2025) 148, https://doi.org/10.1007/s40820-025-01648-w.
[42] F.D. Coms, A.B. LaLonde, C.S. Gittleman, A. Marks, Membrane thickness impact on chemical degradation rates, J. Electrochem. Soc. 172 (2025) 054501, https://doi.org/10.1149/1945-7111/add0e8.
[43] G. Liu, W. Jin, Pervaporation membrane materials: recent trends and perspectives, J. Membr. Sci. 636 (2021) 119557, https://doi.org/10.1016/j.memsci.2021.119557.